Available Power versus Harvested Power in Wind and Solar Energy Systems

Nwosu, C. M., Ogbuka, C. U., Odeh, C. I., Oti, S. E.

Department of Electrical Engineering, University of Nigeria, Nsukka.

Abstract:

The technology for the harnessing of electrical power from renewable resources, for example, solar and wind has continued to improve especially with the deployment of power electronics as interfaces. However, hard nuts still to be cracked is the ability to extract as much power as it is available in the renewable resource. This paper seeks to explore the limits of power extractable from available power in the wind using wind turbine and available power in the solar using photovoltaic (PV) system. From a 20-meter diameter rotor variable speed wind turbine considered in this study, only about 48% of available wind power was extracted. For a case study of 180 PV panels supplying AC power to a common bus through 6 parallel connected inverters located in Electrical Power System Laboratory of Delft University of Technology (TU-Delft), the Netherlands, only about 49% and 77% of available solar power obtained from average solar radiation and PV module data respectively were extracted. The results of these analyses will serve as guides to renewable energy systems planners.

Keywords: *Available power, harvested power, renewable energy, wind turbine, PV system.*

1. Introduction

Wind energy is a solar energy in another form. It is a movement of air around the earth surface, arising from the sun triggered atmospheric changes in temperature and pressure. Theoretically, enormous amount of power resides in wind as well as in solar. Harvesting of electrical power from either of the two forms of renewable energy resources has been a challenge to electrical power producers. Wind energy conversion (WEC) system, consisting majorly of turbine, gear system and generator, is deployed to capture the wind and convert it to electrical power whereas photovoltaic (PV) system is deployed to capture the solar and convert it to electric power. Theoretically, the amount of mechanical power available in wind flow is a function of the cube of the wind speed at that region. This implies that a region with average wind speed of 5.8 m/s and above usually considered good wind resource region has good potential for high wind power whereas a region with average wind speed below 4.5 m/s usually considered a small wind resource region has low potential for adequate wind power [1]. On the other hand, a region for instance Nigeria having latitude and longitude of 10^{o}N and 8^{o} E, with solar insolation closer to that for latitude 0^{o} N has high potential for solar power whereas regions like Russia having latitude of 75^{o} N has low potential for solar power.

However, irrespective of the level of endowment of any region with either of the two sustainable resources, the issue is harvestability in the face of availability. Research has shown that for a WEC system, the harvested power is far less than the available at any given wind speed. Similar result applies also to solar power system at any given solar insolation. This paper, therefore, seeks to analyze this very important phenomenon as it applies to power production by renewable energy resources.

2. Wind Energy System:

The function of a wind turbine is to convert the linear motion of the wind into rotational energy that can be used to drive a generator. Wind turbines capture the power from the wind by means of aerodynamically designed blades and convert it into rotating mechanical power [2]. The principle of operation of a wind turbine encompasses two conversion processes, which are carried out by its two main components: the rotor and the generating system. The rotor extracts kinetic energy from the wind and converts it into a mechanical torque while the generating system converts this torque into electricity [3]. Fig. 1 shows the general principle of operation of wind turbine.

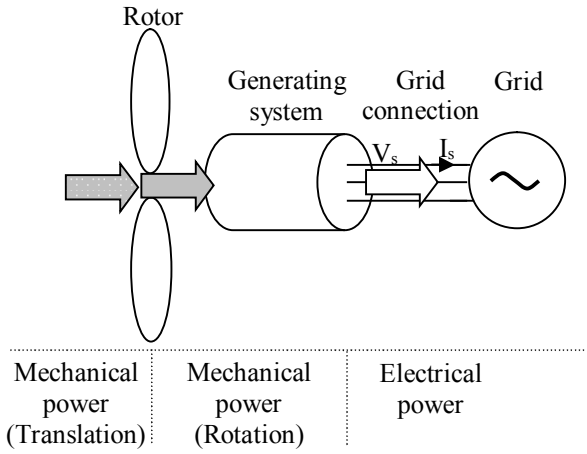

Fig. 1: Diagram of wind power generation.

The mechanical power extracted from the wind [3, 4] is obtained as:

$$P_E = 0.5\rho\pi R^2 V^3 C_p(\lambda) \qquad (1)$$

where P_w is the power extracted from the airflow [W], ρ is the air density (about 1.225 at sea level or 1.168 at standard ambient temperature & pressure) [kg/m3], R is the radius of the turbine blade [m], V is the wind speed upstream of the rotor [m/s], C_p is the turbine power coefficient which represents the power conversion efficiency of a wind turbine, and λ is the tip speed ratio given by:

$$\lambda = \frac{\omega_r R}{V} \qquad (2)$$

where ω_r is the rotor speed.

In practice, wind turbine power depends on both rotor speed and wind speed. For every wind speed, there exists a rotor speed ω_r, at which maximum power can be harvested from a given wind turbine. This maximum power is dependent on the power curve, a plot of power coefficient verses tip-speed ratio. In a variable speed wind turbine where the aerodynamic efficiency of the rotor is reduced by turning the blades out of the wind using hydraulic mechanisms or electric motors, power coefficient $C_p(\theta,\lambda)$ is defined as the ratio of the turbine power to the power of a wind stream of section A [5]. It represents the rotor efficiency of the turbine, and is taken from a lookup table, which contains the specific aerodynamics for a particular turbine. Usually, manufacturer's documentation for a wind turbine includes the turbine power curve. From the power curve, the $C_p(\theta,\lambda)$ is calculated from which the tip-speed ratio can be calculated for each wind speed. The information got from these processes is used to develop an approximation for the $C_p(\theta,\lambda)$ curve. For variable speed wind turbines, the following generic equation [6] may be used to approximate the $C_p(\theta,\lambda)$ curve:

$$C_p(\theta,\lambda) = 0.5176\left(\frac{116}{\lambda_i} - 0.4\theta - 5\right)e^{\frac{-21}{\lambda_i}} + 0.0068\lambda \qquad (3)$$

with

$$\lambda_i = \frac{1}{\frac{1}{\lambda + 0.08\theta} - \frac{0.035}{\theta^3 + 1}} \qquad (4)$$

where θ is the mechanical pitch angle. The aerodynamic model of the wind turbine rotor is based on the $C_p - \lambda$ curve. From the rotor efficiency there is an optimum tip-speed ratio λ^{opt} where the power coefficient is maximum, i.e. $C_p^{max} = C_p(\theta,\lambda^{opt})$, as shown in Fig. 2.

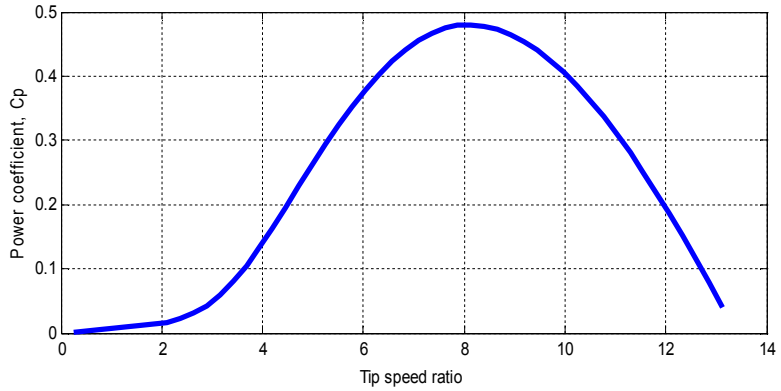

Fig. 2: Typical C_p-λ curve for a 20-m diameter wind turbine at V = 10m/s, and $\theta = 0$.

The electrical output power of the induction generator may be obtained as:

$$P_{el} = \eta_{gen} P_{mec} \qquad (5)$$

where P_{el} is the electrical power and η_{gen} is the generator efficiency.

3.Available Power and Harvested Power at each Wind Speed

The available power in wind turbine varies as the cube of wind speed [4]:

$$P_A = 0.5\rho\pi R^2 V^3 \qquad (6)$$

To investigate the relationship between wind power available at a given wind speed and the harvested power at that wind speed, the power at a 20-meter diameter rotor wind turbine is considered using equation (6) for available power and equation (1) for harvested power. In the investigation of harvested power, zero pitch angle is assumed for the harvested power. Therefore, the performance coefficient depends only on the tip speed ratio and not also on the pitch angle. Maximum power coefficient of 0.39 shall be used. For an assumed 93% efficiency for the wind turbine induction generator, Fig. 3 shows the power variations at different wind speeds. Fig. 4 displays the variations of the extracted power at different wind speeds.

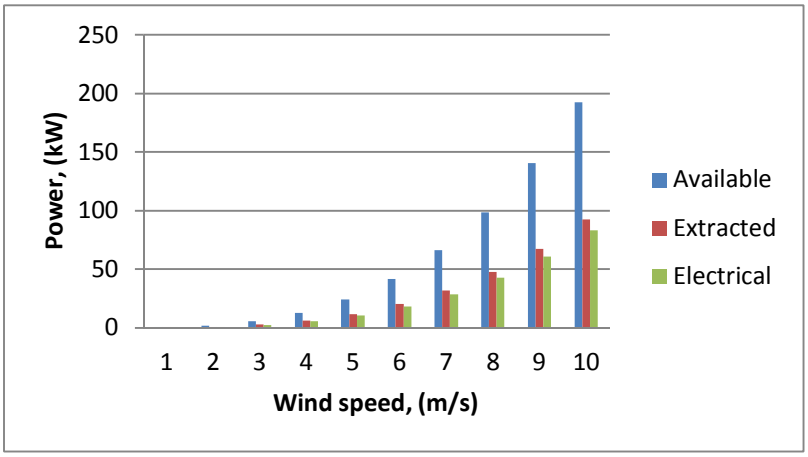

Fig. 3: Chart showing available power, extracted power and electrical powerfor the 20m diameter wind turbine.

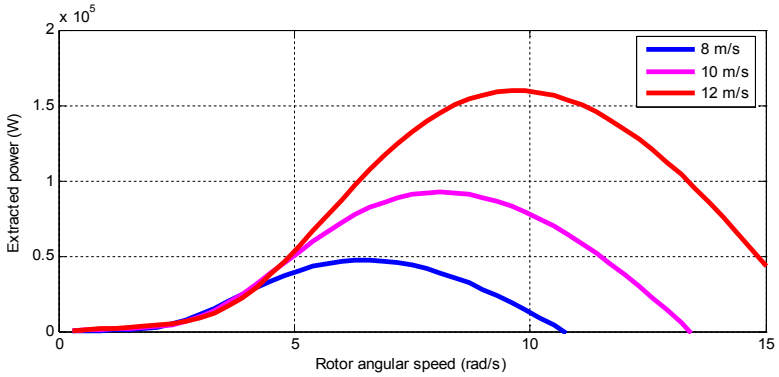

Fig. 4: Harvested power curve for the 20-m diameter wind turbine.

4. Solar Energy System

Outside the atmosphere, the intensity of solar radiation is about 1,300 W/m^2. When this energy is passed through the Earth's atmosphere, photons are scattered and absorbed by particles in the sky, like clouds or haze. Depending on the area, more than 90% of the solar radiation can reach the ground [7]. The available solar radiation in W/m^2 can only be captured and converted to electric power using PV system. The DC power output of the PV may further be synthesized to obtain AC power required by majority of household appliances. The chain of conversions of available solar radiation to AC power comes with series of output degradations in the form of losses such that the harvested power is a fraction of available power.

A relationship which exists between PV module temperature and the amount of power generated by the PV system is such that increase in module temperature leads to decrease in module power. Module operating temperature increases when placed in the sun. As the operating temperature increases, the power output decreases (due to the properties of the conversion material - this is true for all solar modules). The PV Test Condition (PTC) ratings take this into consideration by calculating the PTC ratings based primarily on the specific module temperature characteristics. The PTC ratings are different for each module and can vary from approximately 87%-92% of the Standard Test Conditions (STC) rating. A typical decrease in power output is approximately 12% for crystalline based solar modules. This decrease results in a STC rated 100-Watt DC solar module being PTC rated at approximately 88 Watts DC.

4.1 PV Conversion Chain

Fig. 5 shows PV power conversion chain consisting of paralleled **m** by **n** PV arrays (**m** stands for number of modules in series while **n** is for the number of strings in parallel) usually connected to an inverter. In a whole PV array, there are several strings in parallel.

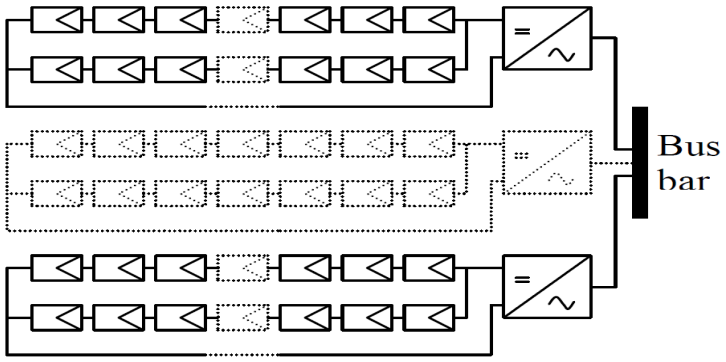

Fig. 5: PV power conversion chain.

A string consists of several PV modules in series. Series wiring increases voltage while parallel wiring increases capacity.

The current–voltage characteristic equation (I–V) of PV arrays is based on the Shockley equation for a diode [8]:

$$I = I_o\left[\exp\left(\frac{qV}{kT}\right)-1\right] \qquad (7)$$

but including other parameters to better describe the measured data from the PV array we have:

$$I_{PV} = n_{ph}I_{ph} - n_p I_{rs}\left[\exp\left(\frac{q\left(V+R_s.I\right)}{A.n_s.k.T}\right)-1\right] - \frac{V+R_s.I}{R_{sh}} \qquad (8)$$

where I is the PV array output current (A), V is the PV array output voltage (V), ns is the number of cells in series, n_p is the number of strings connected in parallel, q is the charge of an electron, k is Boltzmann's constant, A is a p-n junction ideality factor, T is the cell temperature (K), I_{ph} is the cell photo current, I_{rs} is the cell reverse saturation current (A), R_S is the series resistance (Ω), and R_{sh} is the shunt resistance (Ω) [8]. The factor A determines the cell deviation from the ideal p-n junction characteristics. The ideal value ranges between 1 and 5. These data will be evaluated using the values for the short circuit current, open circuit voltage and maximum power point of the I–V characteristic given by the manufacturer. The cell reverse saturation current Irs varies with temperature according to the following equation:

$$I_{rs} = I_{rr}\left[\frac{T}{T_r}\right]^3 \exp\left(\frac{qE_G}{kQA}\left[\frac{1}{T_r}-\frac{1}{T}\right]\right) \qquad (9)$$

where Q is the electron charge, T_r is the cell reverence temperature, I_{rr} is the reverse saturation current at T_r, and E_G is the band-gap energy of the semiconductor in the cell. The photocurrent I_{ph} depends on the solar radiation and the cell temperature as shown in the following equation:

$$I_{ph} = \left[I_{scr} + k_i\left(T-T_r\right)\right]\frac{S}{100} \qquad (10)$$

where I_{scr} is the cell short-circuit current at reference temperature and radiation, k_i is the short-circuit current temperature coefficient, and S is the solar radiation in mW/cm^2.

4.2 Modeling of losses in PV Array

Modeling and analysis of PV array is important in order to approximately account for the losses in the PV array. To achieve this, the PV array is divided into stages. The first stage

is modeling a cell, second is about a module, third is about a string, and the last stage is modeling the whole array. The voltage V_{PVA} of the PV array is:

$$V_{PVA} = N_{PVS}.V_{PV} \quad (11)$$

and the power output P_{PVA} of the PV array is:

$$P_{PVA} = N_{PVP}.N_{PVS}.V_{PV}.I_{PV}.F_{con}.F_{oth} \quad (12)$$

where N_{PVS} is the serial connection number of the PV modules; N_{PVP} is the parallel connection number of the PV module strings; and F_{con} and F_{oth} are the factors representing connection loss and other losses such as the loss caused by accumulative dust, etc.

In this analysis, the PV inverters are regarded as integral part of the PV power unit since the PV arrays and the inverters combine to supply AC power to a common bus. Usually PV array is mounted on roof tops several meters from the inverters and the point of utilization of the power. Three stages of losses considered here are PV array losses, line losses, and inverter losses. The total array losses are modeled by Z_{PV}, losses in line inductance L_L and resistance R_L, may be modeled by Z_L, while inverter losses are modeled by Z_I. Fig. 6 shows a model block diagram representation of the losses.

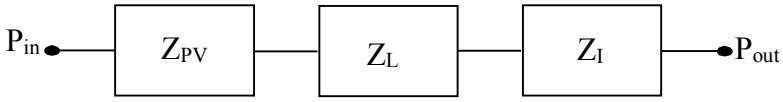

Fig. 6: A Model of Losses in PV/Inverter System.

Switching losses and losses due to non-ideal components result in increase in temperature in the converter systems.

At Standard Test Conditions, a factor known as DC to AC derate factor, which accounts for the losses and efficiencies of components of a PV system is considered. In most cases, the overall default value of plus or minus 0.77 is used to provide a reasonable estimate for modeling the energy production. The components that constitute a whole PV system include [9] PV module nameplate DC rating, inverter and transformer, mismatch, diodes and connections, DC wiring, AC wiring, soiling, system availability, shading, sun-tracking, and age.

To investigate the available power versus extracted power in a PV system, the extracted power is generated from 180 PV panels supplying AC power to a common bus through 6 parallel connected inverters located in Electrical Power System Laboratory of Delft University of Technology (TU-Delft), the Netherlands were studied. Two strings of panels are connected in parallel to each inverter, with each string having a total of 15 modules in

series. The 6 inverters are connected in parallel to the asymmetric bus supplying green power to about 15 households in a developed economy. The available power is derived from the nameplate data of the PV modules as shown in Table 1.The available power is determined from Equation (12) without the loss factors.

To determine the level of power output from the PV array and the percentage of this power the inverters were capable of delivering to the bus, data which included the temperatures of both the inverters and the PV array were recorded over 60 minutes at 10 minutes intervals. Table 2 shows the data from the PV array which included the total power calculated using the measured PV power per square meter and the area of each PV module 51cm by 114cm. Table 3 shows the data from the inverters which include average temperatures and power output of the inverters.

Table 1: PV module data

Open circuit voltage (V_{oc})	21.3V
Short-circuit current (I_{sc})	4.4A
Maximum power	68W
Maximum voltage (V_p)	16.5V
Tolerance on peak power	±4%

Table 2: PV array data

Step	Temperature (°C)	Total power (W)
1	34.921	2309.04
2	28.262	2809.08
3	30.825	7928.00
4	32.877	10050.84
5	33.291	8862.12
6	33.615	9991.08

Table 3: Inverter data

Step	Temperature (°C)	Total power (W)
1	56.8	1937
2	52.7	2276

3	59.5	7368
4	60.0	9361
5	58.8	7955
6	59.0	9007

The available power will be computed under two scenarios. In the first scenario, the 4.67 kWh/m^2/day average solar radiation of Netherlands is converted to kW for the sixty minutes interval under consideration. In the second scenario, the PV module data provided in Table 1 from which 15 by 12 PV array was formed for the case study, is used for the computation of the available power utilizing equation (12) without the loss terms. Fig. 7 displays the variations of the available power (available1 from the first scenario and available2 from the second scenario), extracted power and electrical power. In practice, the available power will vary with time and season; it is nonetheless represented as constant quantity in this scenario. Temperature variations in the PV and the inverter within the 60 minutes interval are displayed in Fig. 8.

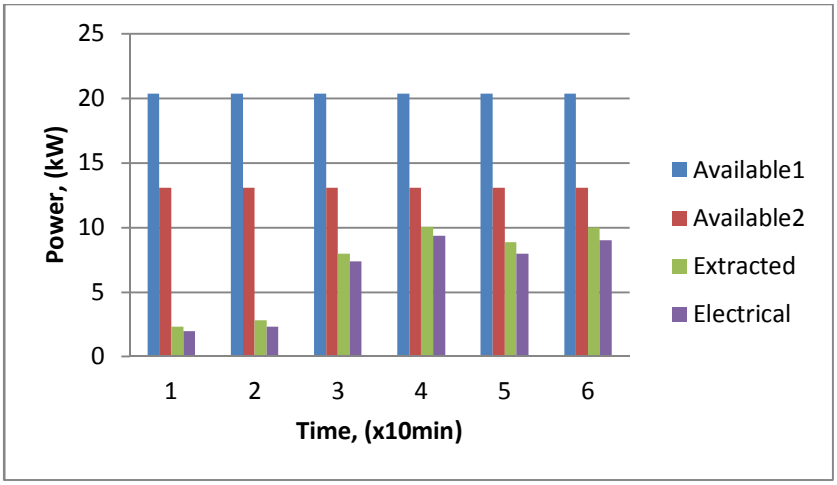

Fig. 7: Chart showing available power, extracted power and electrical powerfor the 20m diameter wind turbine.

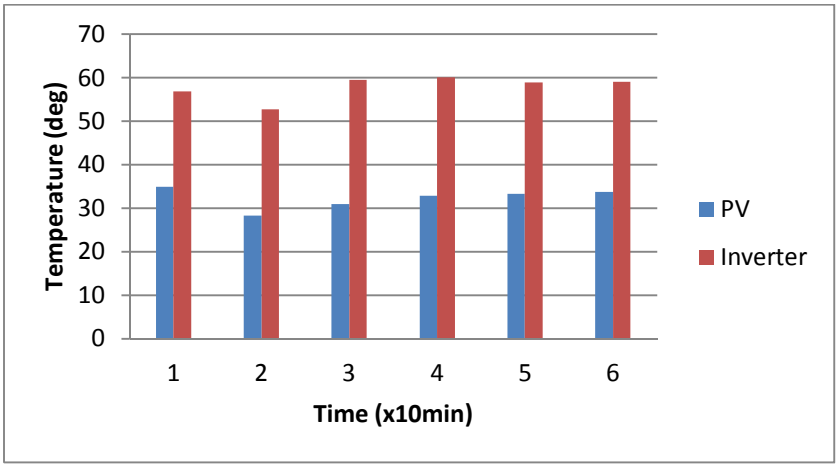

Fig. 8: Chart showing temperature variations in PV and inverter within the 60 minutes interval.

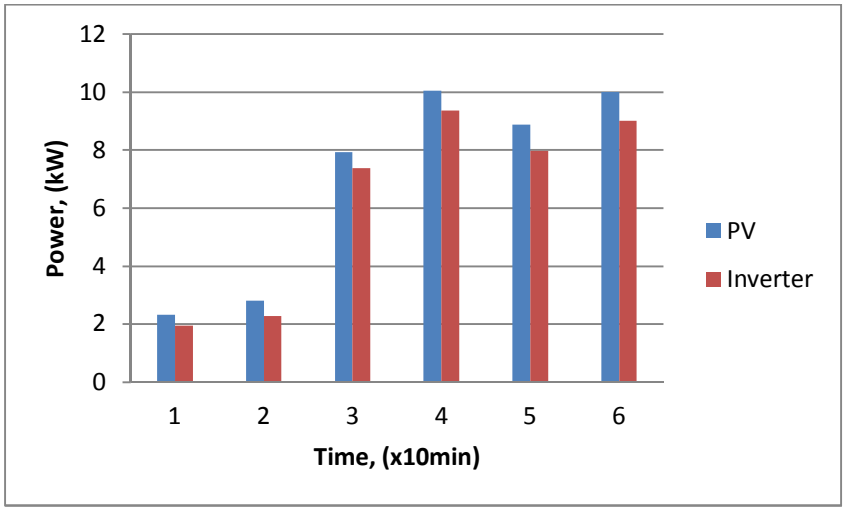

Fig. 9: Chart showing power variations in PV and inverter within the 60 minutes interval.

5. Discussion of results

In this paper, the amount of power that can be extracted from the available power in the wind and in the solar has been explored and presented. Wind turbine and PV system are the two devices for the extractions of power in the wind and solar respectively. The available power in wind turbine varies as the cube of wind speed. However, owing to a factor of power conversion efficiency of a wind turbine usually referred to as power coefficient, only a percentage of the available power can be extracted and then converted to electrical power. For the variable speed wind turbine considered in this paper where the aerodynamic efficiency of the rotor is reduced by turning the blades out of the wind using hydraulic mechanisms or electric motors, only about 48% of the available power can be extracted. Depending on the efficiency of the inverter, the electrical power supplied to a load or connected to the grid as the case may be is further devalued as indicated in Fig. 3. The traces of the extracted power of the wind turbine at three different wind speeds as a result of the power coefficient are shown in Fig. 4 for a 20m diameter wind turbine.

In the Netherlands, used as a case study, the average solar radiation is about 4.67 kWh/m^2/day. This gives about 20.36 kW available power for the 60 minutes period considered in this analysis. Utilizing the PV module data, the available power of about 13.07 kW was realized. From the analysis, only about 49% and 77% of available solar power obtained from average solar radiation and PV module data respectively were extracted. Again, depending on the efficiency of the inverter, the electrical power is further devalued as indicated in Fig. 7. Fig. 8 shows the temperature variations in PV and inverter while Fig. 9 shows the power variations in the PV and in the inverter. From Fig. 8 and Fig. 9, it is observed that while the temperature of the inverters is higher than the temperature of the PV

modules (even though the modules are in direct contact with the sun) the electrical power from the inverter is lower than the extracted power from the PV arrays.

6. Conclusions

The limits of extractable power from available power in the wind using wind turbine and available power in the solar using photovoltaic (PV) system has been presented. In exploring the percentage of extractable power from available power in the wind, a 20-meter diameter rotor variable speed wind turbine was considered. For solar system, a case study of 180 PV panels supplying AC power to a common bus through 6 parallel connected inverters located in Electrical Power System Laboratory of Delft University of Technology (TU-Delft), the Netherlands was considered. It was established for the wind turbine that only about 48% of available wind power could be extracted while for the solar system, only about 49% and 77% of available solar power obtained from average solar radiation and PV module data respectively could be harvested. The results of these analyses will serve as guides not only to renewable energy systems planners but also to home owners and industrialists who may wish to invest in distributed power generation to meet specific needs especially where utility grid is far from load centers.

7. References

[1] Hybrid Power Systems – Issues & Answers, Available Online *03-08-2011*: http://photovoltaics.sandia.gov/docs/Hybook.html

[2] F. Blaabjerg, R. Teodorescu, Z. Chen, and M. Liserre, ‘’Power Converters and Control of Renewable Energy Systems,’’….

[3] J. G. Slootweg, *Wind Power Modeling and Impact on Power System Dynamics*, PhD Thesis, DelftUniversity of Technology, (TU-Delft), the Netherlands, 2003.

[4] P. W. Carlin, A. S. Laxson, and E. B. Muljadi, ‘’The History and State of the Art of variable-Speed Wind Turbine Technology,’’ National Renewable Energy laboratory, 1617 Cole Boulevard, Golden, Colorado, Feb. 2001.

[5] B. Pokharel, *Modeling, Control and Analysis of a Doubly Fed Induction Generator Based Wind Turbine System with Voltage Regulation,*Msc. Thesis, TennesseeTechnicalUniversity, 2011.

[6] N. Rumzi, N. Idris, and H. M. Yatim, “An Improved Stator Flux Estimation in Steady-State Operation for Direct Torque Control of Induction Machines,” IEEE Trans. Ind. Applicat. vol. 38, pp. 110 – 116, Jan/Feb. 2002.

[7] Shahidehpour, M. and F. Schwarts. 2004. “Let the Sun go Down on PV [photovoltaic system]”. *IEEE Power and Energy Magazine*. 2(3):40 – 48.

[8] Shahidehpour, M. and F. Schwarts. 2004. “Let the Sun go Down on PV [photovoltaic system]”. *IEEE Power and Energy Magazine*. 2(3):40 – 48.

[9] Yu, G.J., Y.S. Jung, J.Y. Choi, and G.S. Kim. 2004. “A Novel Two-Mode MPPT Control Algorithm Based on Comparative Study of Existing Algorithms”. *Science Direct – Solar Energy*. 76(4):455 – 463.